



Orientation-dependent recrystallization in an oxide dispersion strengthened steel after dynamic plastic deformation

Zhang, Zhenbo; Tao, N.R.; Mishin, Oleg V.; Pantleon, Wolfgang

Published in:

I O P Conference Series: Materials Science and Engineering

Link to article, DOI:

[10.1088/1757-899X/89/1/012059](https://doi.org/10.1088/1757-899X/89/1/012059)

Publication date:

2015

Document Version

Publisher's PDF, also known as Version of record

[Link back to DTU Orbit](#)

Citation (APA):

Zhang, Z., Tao, N. R., Mishin, O. V., & Pantleon, W. (2015). Orientation-dependent recrystallization in an oxide dispersion strengthened steel after dynamic plastic deformation. *I O P Conference Series: Materials Science and Engineering*, 89, [012059]. <https://doi.org/10.1088/1757-899X/89/1/012059>

General rights

Copyright and moral rights for the publications made accessible in the public portal are retained by the authors and/or other copyright owners and it is a condition of accessing publications that users recognise and abide by the legal requirements associated with these rights.

- Users may download and print one copy of any publication from the public portal for the purpose of private study or research.
- You may not further distribute the material or use it for any profit-making activity or commercial gain
- You may freely distribute the URL identifying the publication in the public portal

If you believe that this document breaches copyright please contact us providing details, and we will remove access to the work immediately and investigate your claim.

Orientation-dependent recrystallization in an oxide dispersion strengthened steel after dynamic plastic deformation

This content has been downloaded from IOPscience. Please scroll down to see the full text.

2015 IOP Conf. Ser.: Mater. Sci. Eng. 89 012059

(<http://iopscience.iop.org/1757-899X/89/1/012059>)

View [the table of contents for this issue](#), or go to the [journal homepage](#) for more

Download details:

IP Address: 192.38.90.17

This content was downloaded on 11/08/2015 at 10:12

Please note that [terms and conditions apply](#).

Orientation-dependent recrystallization in an oxide dispersion strengthened steel after dynamic plastic deformation

Z B Zhang^{1,4}, N R Tao^{2,4}, O V Mishin^{1,4} and W Pantleon^{3,4}

¹ Section for Materials Science and Advanced Characterization, Department of Wind Energy, Technical University of Denmark, Risø Campus, 4000 Roskilde, Denmark

² Institute of Metal Research, Chinese Academy of Science, Shenyang 110016, China

³ Section for Materials and Surface Engineering, Department of Mechanical Engineering, Technical University of Denmark, 2800 Kgs. Lyngby, Denmark

⁴ Sino-Danish Center for Education and Research

E-mail: zhenbo.zhang@manchester.ac.uk

Abstract. The microstructure of the oxide dispersion strengthened ferritic steel PM2000 has been investigated after compression by dynamic plastic deformation to a strain of 2.1 and after subsequent annealing at 715 °C. Nanoscale lamellae, exhibiting a strong $\langle 100 \rangle + \langle 111 \rangle$ duplex fibre texture, form during dynamic plastic deformation. Different boundary spacings and different stored energy densities for regions belonging to either of the two fibre texture components result in a quite heterogeneous deformation microstructure. Upon annealing, preferential recovery and preferential nucleation of recrystallization are found in the $\langle 111 \rangle$ -oriented lamellae, which had a higher stored energy density in the as-deformed condition. In the course of recrystallization, the initial duplex fibre texture is replaced by a strong $\langle 111 \rangle$ fibre recrystallization texture.

1. Introduction

Oxide dispersion strengthened (ODS) steels are considered to be promising structural materials for the next-generation fission and fusion reactors because of their excellent resistance to both irradiation damage and high-temperature creep [1,2]. It has been suggested that irradiation induced swelling might be reduced in materials with well-refined microstructures, and that these materials may therefore exhibit improved irradiation tolerance compared to their coarse-grained counterparts [3,4]. One way to refine the microstructure is via plastic deformation when original grains are subdivided by deformation-induced dislocation boundaries [5].

In previous studies [6,7], dynamic plastic deformation (DPD) at high strain rates (10^2 - 10^3 s⁻¹) [8] has been demonstrated to be more efficient in refining the microstructure of a ferritic/martensitic steel than deformation at low strain rates. In the present work, the microstructure and the texture of a ferritic ODS steel PM2000 are investigated after DPD to a strain of 2.1. As the service temperatures of ODS steels in reactors are expected to be rather high, the thermal stability of the microstructure obtained by DPD is analysed focusing on orientation-dependent recovery and recrystallization taking place during annealing.



2. Experimental

A ferritic steel PM2000 (see Table 1) with oxide nanodispersoids was received in the form of a hot-extruded rod with a diameter of 13 mm [9]. Cylindrical specimens with a diameter of 6 mm and height of 9 mm were machined with their cylinder axis along the extrusion direction. The specimens were compressed by 5 passes at room temperature by DPD at a strain rate of $10^2 - 10^3 \text{ s}^{-1}$ to an equivalent strain of 2.1 [10]. The deformed material was then annealed isothermally at 715 °C for different durations.

Table 1. Nominal chemical composition (wt. %) of PM2000 [10].

Cr	Al	Ti	Y ₂ O ₃	Fe
20	5.5	0.5	0.5	Bal.

The microstructure of the deformed and annealed samples was investigated by electron backscatter diffraction (EBSD) in a Zeiss Supra 35 FEGSEM equipped with a Channel 5 system. Due to the limited angular resolution of the EBSD technique [11,12], misorientation angles θ less than 2° were not considered in the analysis. Boundaries with misorientation angles θ between 2° and 15° were defined as low angle boundaries (LABs), while boundaries with misorientation angles θ larger than 15° were classified as high angle boundaries (HABs). The volume fraction of the different texture components were calculated allowing a 10° orientation deviation from the exact $\langle 100 \rangle$ and $\langle 111 \rangle$ fibres.

The recrystallized volume fraction was determined by identifying individual recrystallized grains as regions at least partly surrounded by HABs, having an equivalent circular diameter (ECD) above 3 µm and an internal point-to-point misorientation below 2° [13]. The boundary area density S_V was determined from the EBSD data [14] and the energy density stored in the form of boundaries in the deformed or recovered microstructure was calculated as $u = \gamma S_V$. The surface energy of HABs was assumed to be $\gamma_{\text{HAB}} = 617 \text{ MJ/m}^2$ [15], whereas the surface energy of LABs with misorientation angles $\theta < \theta_{\text{cr}} = 15^\circ$ was calculated using the Read-Shockley equation [16]:

$$\gamma_{\text{LAB}} = \gamma_{\text{HAB}} \frac{\theta}{\theta_{\text{cr}}} \left(1 - \ln \left(\frac{\theta}{\theta_{\text{cr}}} \right) \right) \quad (1)$$

3. Results

The orientation map obtained by EBSD (figure 1a) from PM2000 after DPD to a strain of 2.1 shows a nanoscale deformation structure with lamellar boundaries almost perpendicular to the compression axis (CA). The microstructure is substantially refined by DPD as is evident from the spacing $d_{\theta > 2^\circ}$ measured along the CA between boundaries with $\theta > 2^\circ$, which decreased from 580 nm in the as-received material to 76 nm after DPD (see table 2). The fraction of LABs (f_{LAB}) in this deformed microstructure is 52%. It is apparent that the map contains mainly two types of regions which appear either in red or in blue, corresponding to $\langle 100 \rangle$ and $\langle 111 \rangle$ fibre texture components, respectively.

The microstructural evolution during annealing after DPD is illustrated by orientation maps for the samples annealed at 715 °C for 10, 20, and 80 min (figure 1b-d). It is seen that the lamellar morphology observed in the as-deformed material is retained after 10 min of annealing (figure 1b). The fraction of LABs after 10 min of annealing is similar to that in the as-deformed condition (see table 2). However, during annealing the microstructure coarsens and the average spacing $d_{\theta > 2^\circ}$ increases from 76 nm in the DPD sample to 176 nm after 10 min at 715 °C. The material is still mainly in the recovered state, with only a single recrystallization nucleus found in the characterized area, which accounts for 1% of the volume fraction. After 20 min of annealing, the volume fraction of recrystallized material (f_{rex}) is 68% and the average boundary spacing $d_{\theta > 2^\circ}$ is 750 nm. After annealing

for 80 min, the material is almost fully recrystallized ($f_{\text{rex}}=97\%$) with $d_{\theta>2^\circ} = 3750$ nm. The fraction of LABs in this almost fully recrystallized microstructure is only 19% (cf. table 2).

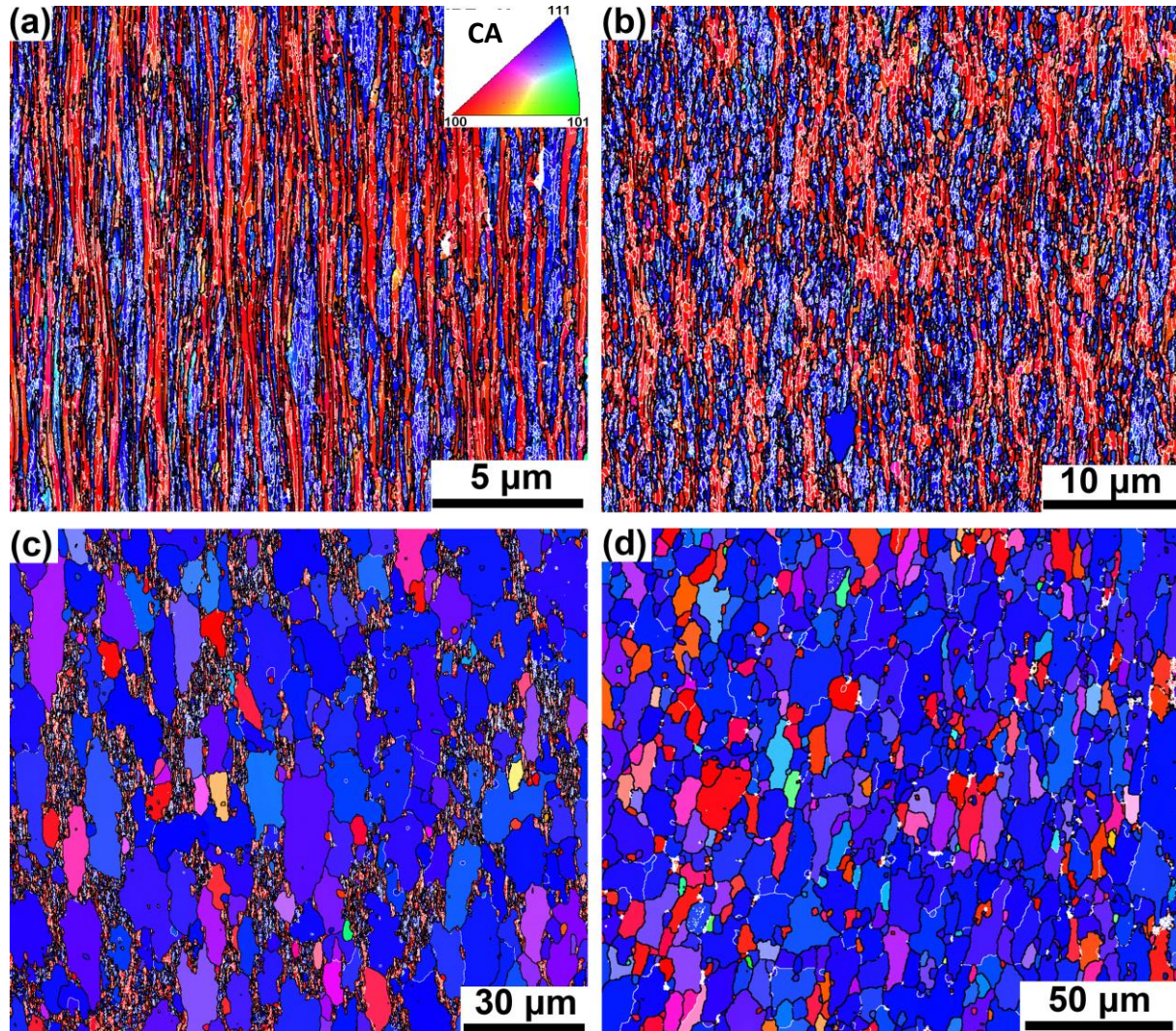


Figure 1. Orientation map obtained by EBSD from the longitudinal section of PM2000: (a) after compression by DPD to a strain of 2.1, and after subsequent isothermal annealing at 715 °C for (b) 10 min, (c) 20 min and (d) 80 min. The maps are coloured according to the crystallographic direction along the CA (see the inset). Black and white lines represent HABs and LABs, respectively. The CA is horizontal.

Table 2. Microstructural parameters of PM2000 after DPD and subsequent annealing at 715 °C.

Annealing duration (min)	$d_{\theta>2^\circ}$ (nm)	f_{rex} (%)	f_{LAB} (%)
0	76	0	52
10	176	1	54
20	750	68	47
80	3750	97	19

The orientation maps provide evidence that the majority of recrystallized grains have a $\langle 111 \rangle$ direction along the CA (blue in figure 1b-d). In the sample annealed for 80 min (figure 1d), such $\langle 111 \rangle$ -oriented grains occupy 67% of the area. The evolution of crystallographic texture is further illustrated by the inverse pole figures in figure 2. It is seen that the $\langle 100 \rangle + \langle 111 \rangle$ duplex fibre texture in the as-deformed PM2000 evolves during annealing into a well-defined $\langle 111 \rangle$ fibre texture, whereas the strength of the $\langle 100 \rangle$ fibre texture component decreases gradually. From the volume fractions of the individual texture components in figure 3 it is apparent that during recrystallization the $\langle 111 \rangle$ fibre strengthens primarily at the expense of the $\langle 100 \rangle$ fibre, i.e. recrystallization in PM2000 after compression by DPD is orientation-dependent.

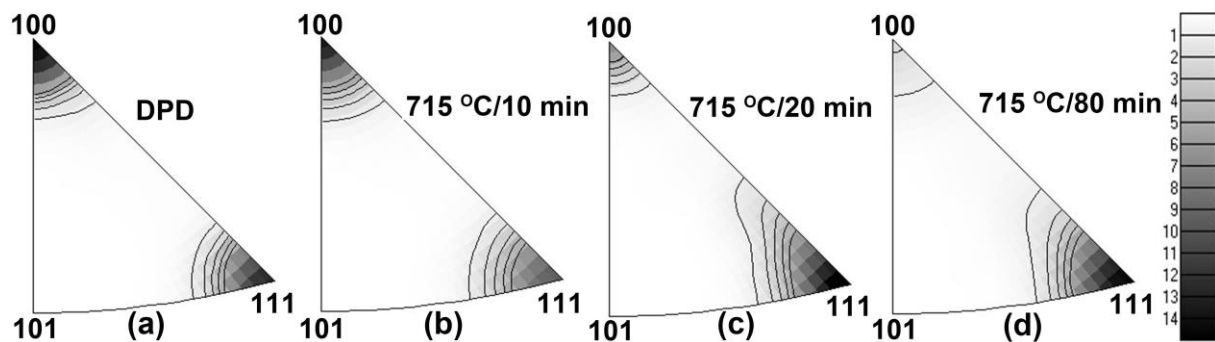


Figure 2. Inverse pole figures representing the crystallographic directions parallel to the CA in PM2000: (a) after compression by DPD to a strain of 2.1, and after subsequent isothermal annealing at 715 °C for (b) 10 min, (c) 20 min and (d) 80 min.

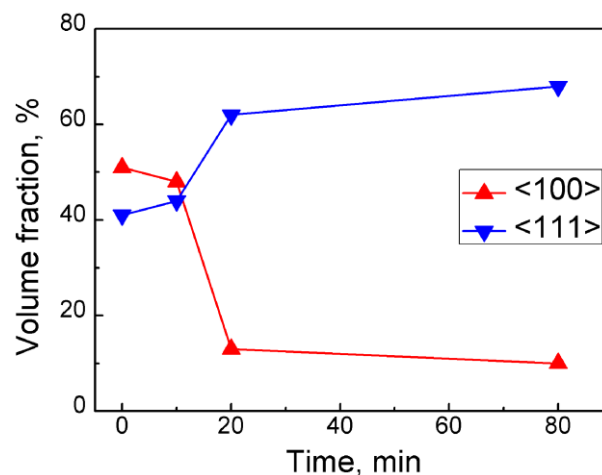


Figure 3. Volume fractions of the $\langle 100 \rangle$ and $\langle 111 \rangle$ fibre texture components in PM2000 after compression by DPD to a strain of 2.1 and subsequent isothermal annealing at 715 °C.

4. Discussion

Compression of PM2000 by DPD to a strain of 2.1 results in nanoscale lamellar structures with a boundary spacing of 76 nm as determined by EBSD along the CA. This spacing is considerably smaller than the value of 110 nm obtained in a modified 9Cr-1Mo steel compressed by DPD to a similar strain [7]. The smaller spacing in PM2000, as compared to the modified 9Cr-1Mo steel, is attributed to the finer starting microstructure as well as the enhanced structural refinement due to the oxide nanodispersoids in PM2000.

The lamellar structure shows a strong $\langle 100 \rangle + \langle 111 \rangle$ duplex fibre texture, which is in agreement with earlier reports on textures developing during free compression in body centred cubic materials [6,7,17-19]. The development of such a duplex fibre texture can be rationalized in terms of Taylor-type models based on $\langle 111 \rangle$ -pencil glide of dislocations in body centred cubic materials [20].

During annealing, lamellae of the different fibre texture components exhibit very different recrystallization behaviour, with the majority of the recrystallized grains belonging to the $\langle 111 \rangle$ fibre. This orientation-dependent recrystallization leads to a dominant $\langle 111 \rangle$ fibre texture in the recrystallized material. This texture evolution during recrystallization of PM2000 is similar to that previously observed during annealing of heavily compressed iron [18,19].

To understand the reason for the observed differences in the annealing behaviour of regions having different orientations, structural parameters of the deformed and recovered material in the present PM2000 sample were analysed separately for the two different texture components (see figure 4). Figure 4a demonstrates that after DPD the boundary spacing $d_{\theta > 2^\circ}$ within the $\langle 100 \rangle$ -oriented lamellae is larger (80 nm) than that within the $\langle 111 \rangle$ -oriented lamellae (68 nm). After 10 min of annealing, however, this difference becomes smaller, while after 20 min of annealing, $d_{\theta > 2^\circ}$ of the $\langle 111 \rangle$ -oriented lamellae is even larger than that of the $\langle 100 \rangle$ -oriented lamellae (note that for partially recrystallized samples, the reported spacings $d_{\theta > 2^\circ}$ represent only recovered regions). Figure 4b shows the stored energy density u calculated from the EBSD data for the $\langle 100 \rangle$ - and $\langle 111 \rangle$ -oriented regions in the deformed and annealed samples. It is seen that in the deformed microstructure $u_{\langle 111 \rangle}$ is considerably higher than $u_{\langle 100 \rangle}$. This difference, however, becomes very small after 10 min at 715 °C (see figure 4b). After annealing at 715 °C for 20 min $u_{\langle 111 \rangle}$ is even somewhat lower than $u_{\langle 100 \rangle}$.

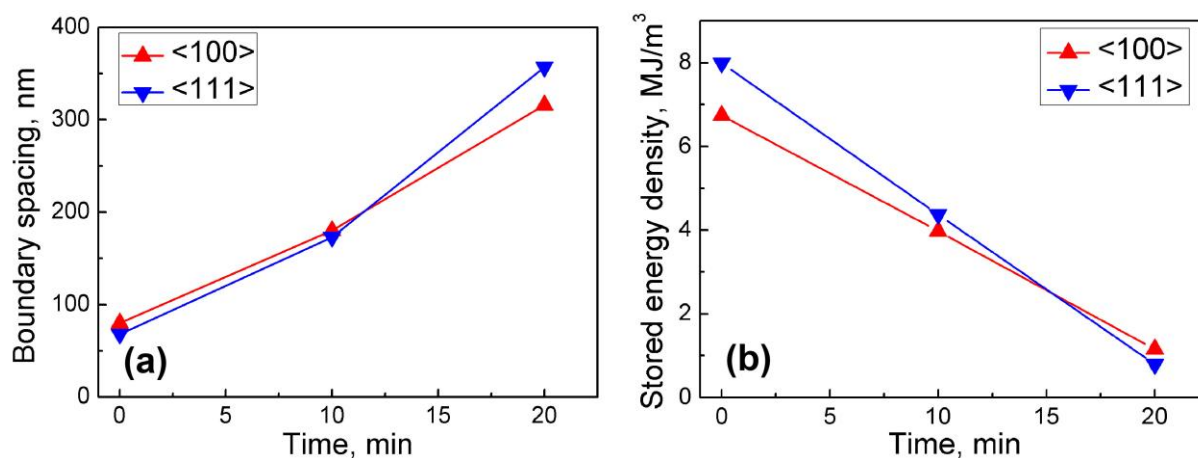


Figure 4. Evolution of structural parameters during recovery of PM2000 compressed by DPD to a strain of 2.1: (a) the average boundary spacing between boundaries with misorientation angles θ above 2° measured along the CA; (b) the stored energy density for the $\langle 100 \rangle$ and $\langle 111 \rangle$ fibre texture components. Both parameters are determined from the EBSD data for the deformed and recovered regions only.

The differences between the $\langle 100 \rangle$ - and $\langle 111 \rangle$ -oriented lamellae in the deformed microstructure are attributed to the difference in their Taylor factors during compression. Assuming pencil glide, the Taylor factor for body centred cubic crystals compressed along $\langle 100 \rangle$ is 2.1, while for compression along $\langle 111 \rangle$, the Taylor factor is 3.2 [21] which are respectively the lowest and highest values among all directions. This considerable difference between the two fibre texture components indicates that during compression, regions of the $\langle 111 \rangle$ component experience appreciably larger plastic slip than regions of the $\langle 100 \rangle$ component. Consequently, the work done to deform individual grains with a higher Taylor factor is larger than that to deform grains with a lower Taylor factor. Therefore, the

stored energy density can also be expected to be larger in regions with a higher Taylor factor. It is believed that this higher stored energy in $\langle 111 \rangle$ -oriented lamellae results in faster recovery (as seen in the faster reduction of the stored energy in figure 4b), also leading to preferential nucleation in these $\langle 111 \rangle$ -oriented regions.

5. Conclusion

Compression by DPD to a strain of 2.1 significantly refines the initial microstructure of PM2000, resulting in nanoscale lamellae with a $\langle 100 \rangle + \langle 111 \rangle$ duplex fibre texture. Orientation-dependent recrystallization takes place during annealing at 715 °C leading to strengthening of the $\langle 111 \rangle$ fibre texture component primarily at the expense of the $\langle 100 \rangle$ fibre texture component. As a result, a strong $\langle 111 \rangle$ fibre texture is present when recrystallization is almost complete. It is suggested that this orientation-dependent recrystallization is caused by a higher stored energy in the $\langle 111 \rangle$ -oriented lamellae after DPD. During annealing these lamellae recover faster than lamellae of the $\langle 100 \rangle$ fibre texture component, which possibly causes the observed preferential nucleation of $\langle 111 \rangle$ -oriented grains.

Acknowledgements

Financial support from the Sino-Danish Center for Education and Research is gratefully acknowledged. The authors are grateful to Prof. M. Heilmaier for providing the initial PM2000 sample. OVM also gratefully acknowledges the support from the Danish National Research Foundation (Grant No. DNRF86-5) and the National Natural Science Foundation of China (Grant No. 51261130091) to the Danish-Chinese Center for Nanometals.

References

- [1] Odette G R, Alinger M J and Wirth B D 2008 *Ann. Rev. Mater. Res.* **38** 471
- [2] Chant I and Murty K L 2010 *JOM* **62** 67
- [3] Bai X M, Voter A F, Hoagland R G, Nastasi M and Uberuaga B P 2010 *Science* **327** 1631
- [4] Song M, Wu Y D, Chen D, Wang X M, Sun C, Yu K Y, Chen Y, Shao L, Yang Y, Hartwig K T and Zhang X 2014 *Acta Mater.* **74** 285
- [5] Hansen N 2006 *Metall. Mater. Trans. A* **32** 2917
- [6] Zhang Z B, Mishin O V, Tao N R and Pantleon W 2015 *Mater. Sci. Technol.* **31** 715
- [7] Zhang Z B, Mishin O V, Tao N R and Pantleon W 2015 *J. Nucl. Mater.* **458** 64
- [8] Li Y S, Tao N R and Lu K 2008 *Acta Mater.* **56** 230
- [9] Schneibel J H, Heilmaier M, Blum W, Hasemann G and Shanmugasundaram T 2011 *Acta Mater.* **59** 1300
- [10] Zhang Z B, Mishin O V, Tao N R and Pantleon W 2014 *IOP Conf. Ser.: Mater. Sci. Eng.* **63** 012065
- [11] Humphreys F J 2006 *J. Mater. Sci.* **36** 3833
- [12] Mishin O V, Östensson L and Godfrey A 2006 *Metall. Mater. Trans. A* **37** 489
- [13] Wu G L and Jensen D Juul 2008 *Mater. Charact.* **59** 794
- [14] Godfrey A, Hansen N and Jensen D Juul 2007 *Metall. Mater. Trans. A* **38** 2329
- [15] Humphreys F J and Hatherly M 2004 *Recrystallization and related annealing phenomena* (second edition) (Oxford: Elsevier)
- [16] Read W T and Shockley W 1950 *Phys. Rev.* **78** 275
- [17] Hu H 1974 *Texture* **1** 233
- [18] Dillamore I L, Katoh H and Haslam K 1974 *Texture* **1** 151
- [19] Khatirkar R, Krishna K V M, Kestens L A I, Petrov R, Pant P and Samajdar I 2011 *ISIJ Int.* **51** 849
- [20] Hosford W F 2005 *Mechanical Behavior of Materials* (Cambridge University Press)
- [21] Rosenber J M and Piehler H R 1971 *Metall. Trans.* **2** 257